Control Engineering Practice 95 (2020) 104226

Contents lists available at ScienceDirect

Control Engineering Practice

journal homepage: www.elsevier.com/locate/conengprac

Adaptive estimation of the hydraulic gradient for the location of multiple leaks in pipelines☆

J. Rojas *, C. Verde

Instituto de Ingeniería, Universidad Nacional Autónoma de México, Mexico

ARTICLE INFO

Keywords:
Hydraulic gradient estimation
Multiple leaks in pipelines
Switched estimation scheme
Adaptive observer
Extended Kalman filter
Sliding mode observer

ABSTRACT

A scheme is proposed for detecting and locating multiple sequential leaks, based on a combination of an adaptive observer to identify the hydraulic gradient in real time and a leak location observer to estimate the leak position and its outflow. The main contribution is the use of an equivalent leak model which switches with an identification function for the hydraulic gradient without input excitation. Experimental results of a pilot pipeline showed a satisfactory estimation in spite of operation changes and leaks. Moreover they revealed that if leaks must be located, a precise knowledge of the hydraulic gradient is required.

1. Introduction

Pipelines are an efficient and economic mean of fluid transport. Despite the significant advances of SCADA systems for fluid transportation networks, important problems associated with the modeling, instrumentation, control and monitoring of pipelines and networks have been only partially solved (Farmer, 2017). One of the causes of these problems is that the fluid flows behave differently from the nominal operation range used in the design mainly because of perturbations, uncertainties, deterioration and the aging of the installation. Several reasons are the presence of uncertain roughness, deviations in density and the viscosity of the fluid, the line age, lack of maintenance, light damages and natural phenomena (Islam & Chaudhry, 1998). An important reason that limits the operation and safety of the networks is the difficulty or impossibility in measuring real-time features, such as pipe corrosion or the presence of polluting materials mixed with the main fluid. Moreover, the attributes of a pressurized flow system for homogeneous two-phase flows have seldom been studied in comparison with a one-phase flow (Malekpour & Karney, 2018). These facts have motivated a considerable effort for developing software sensors and estimation capabilities regarding the pipeline operation in real time. Thus, by considering the feasibility of having indirect flow information in pipelines, advanced software tools have been generated by the data processing and control community for the safe operation of pipelines and networks in real-time (Puig, Ocampo-Martínez, Pérez, Cembrano, Quevedo, & Escobet, 2017; Verde, 2017).

In particular for pipeline leakage detection, Datta and Sarkar (2016) described in a very clear report the diverse possibilities that range from manual inspection by trained operators to advanced satellite imaging. Methods are separated into two groups. They are based on specific hardware, such as acoustic reflectometry (Martini, Troncossi, & Rivola, 2017), optic fiber (Huang, Lin, Tsai, & Chen, 2007) and so on. The software methods are based on estimation models, signal processing and artificial intelligence algorithms, which take data from sensors of flow velocity, pressure and temperature. In this group, one can find methods like simulations (Ben-Mansour, Habiib, Kalifa, et al., 2012), negative pressure wave analysis (Brunone & Ferrante, 2001), frequency response (Lee, Vitkovsky, Lambert, Simpson, & Liggett, 2005), and observer tools (Besançon, 2017). Furthermore, Colombo, Lee, and Karney (2009) published a selective set of methods based on the transient response of the flow pressure, but the procedures require maneuvers not acceptable in all practical installations. Few methods have been published related to the case of simultaneous leaks and tested in real conditions. Recently, Lazhar, Hadj-Taïeb, and Hadj-Taïeb (2013), Rui, Han, Zhang, Wang, Pu, and Ling (2017) and Wang (2018) suggested some particular procedures based on static relations, but only simulation tests are presented.

An important result related to the weak isolability of two leaks was reported in Verde (2003), where it is shown that the isolability condition can only be satisfied during the transient response caused by the leaks; otherwise, false leaks are identified. Thus, off-line approaches were proposed to minimize the transient error between models and data for two leaks (as in Verde, Visairo, and Gentil (2007) and Verde, Molina, and Torres (2014)). The performance of these procedures, however, is not always satisfactory in real situations. This inconvenience motivated the reformulation of the problem for leak isolation under the condition of sequential leaks.

☆ Supported by IT100519-PAPIIT-UNAM, and Conv2016-3, Fondo Sectorial CONACyT-Secretaría de Energía-Hidrocarburos, Mexico.
* Corresponding author.
E-mail addresses: jorgeing7@gmail.com (J. Rojas), verde@unam.mx (C. Verde).

https://doi.org/10.1016/j.conengprac.2019.104226
Received 9 February 2019; Received in revised form 31 October 2019; Accepted 3 November 2019
Available online xxxx
0967-0661/

Verde and Rojas (2015) developed a location method for sequential leaks by assuming that only the flow rate and pressure at the ends of the pipeline were measurable. The equivalent input–output model in steady state for one leak and n leaks is used such that each time a new leak occurs only two parameters must be identified in a finite dimensional model. This simple idea allowed the identification of the same structural model each time a new leak was present. The simulations showed satisfactory results for three leaks, but practical results were not satisfactory since the parameters of the hydraulic gradient were uncertain throughout the experiment. Recently, Delgado-Aguiñaga, Besançon, Begovich, and Carvajal (2016) presented the state of art of this type of diagnosis and suggested a model adaptation strategy in which each time a new leak appears, the system dynamic model must be increased; however, the estimation errors increase when the parameters deviate from the nominal values. In addition, high-order sliding mode observers were used to reconstruct unknown outflow rates, but the relative degree condition restricts the applicability to only two outflows. Moreover, despite the assumption of a boundary derivative for the outflow signals, the state estimation with the sliding mode is not robust (Fernández, Verde, & Moreno-Pérez, 2018).

The common assumption of the aforementioned procedures is the invariant of the function caused by the friction between the conduit wall and the flow in any flow conditions. As Verde and Rojas (2017) pointed out, when flows have a Reynolds number lower than 4000 for incompressible fluid and rigid conduit walls, the function could change from the nominal condition under diverse scenarios. The greater the number of uncertain parameters and the deviation of the nominal value caused by the leaks, the greater the position error will be.

As a consequence, the robustness of any leak diagnosis is affected when the hydraulic gradient is not exactly known. This justifies the estimation of the friction factor in real time, as suggested by Billman and Isermann (1987), before the leak occurrence. On the other hand, the authors of Dulhoste, Besançon, Torres, et al. (2011) have shown that for leak diagnosis a variable friction without nonstationary losses is an appropriate formulation.

In the recent past, diverse functions using observer schemes with an input excitation condition have been proposed to identify the hydraulic gradient in real time. For example, Torres and Verde (2018) proposed a power law for this function. Since the excitation signal is not always allowed for security reasons in a real hydrocarbon installation, this proposition cannot be applied permanently.

Thus, an accurate diagnosis system for pipeline monitoring requires the update of the hydraulic gradient permanently. This remark takes importance for the case of multiple leaks since each new leak slowly produces changes in this function.

The above facts motivated this work to design an accurate location scheme for sequential leaks, which is based on a residual that generates commutation on-line between two observers each time a new leak must be estimated. One adaptive observer, according to Besançon (2007), is applied only for identifying the parameters of the hydraulic gradient during the detection stage, and the second observer estimates the equivalent leak position and its piezometric head by assuming that the parameter of the hydraulic gradient is constant during the leak location time. An extended Kalman filter (EKF) or a Sliding Mode Observer (SMO) are suggested for the second observer. Thus, one observer calculates the slow deviations of the hydraulic gradient (J_s) when the residual is off, and the other observer precisely locates the equivalent leak position by using the loss function previously estimated. The key to the simple switched scheme is the application of a structure for both observers with different estimation tasks, and is the main contribution of the paper. Advantages of this scheme are that the dynamic model does not increase with the number of leaks and that no input excitation is required.

The paper is organized as follows. Section 2 introduces the equivalent leak input–output model that is used for both estimation tasks. Section 3 describes the real-time scheme for the location of multiple leakages with an update of the hydraulic gradient to reduce the location error. The design is based on two real-time independent estimation tasks commutated by a residual and the equivalence relation between the input–output models with one leak and n leaks. This functions combination improves the precision of the leak location, and it is the main contribution of the paper. Section 4 discusses the performance of the scheme with experimental data from a hydraulic pilot pipeline at the UNAM where two sequential leaks were emulated. Finally, it is concluded in Section 5 that the new scheme improves the accuracy of the location for sequential leaks with respect to the method reported in Verde and Rojas (2017).

2. Model for a pressurized pipe with leaks

2.1. Minimum-order transient flow model

The transient flow model in pressurized pipes is based on the conservation rules of momentum and mass that govern transient flows. Thus, the partial differential equation model for a straight section of a one-dimension section can be written by

$$\begin{aligned} \frac{1}{a_1}\frac{\partial Q(z,t)}{\partial t}+\frac{\partial H(z,t)}{\partial z}+J_s(Q(z,t),\wp)=0,\\ \frac{\partial H(z,t)}{\partial t}+a_2\frac{\partial Q(z,t)}{\partial z}=0, \end{aligned} \tag{1}$$

where $H(z,t)$ and $Q(z,t)$ respectively, denote the piezometric pressure head and flow rate at the center of the pipe, L as the length of the pipe, $z\,\epsilon\,[0,L]$ as the position variable and $t\geq 0$ as the time variable. Furthermore, $a_2 = b^2/a_1$ with b as the fluid pressure wave speed, $a_1 = gA_r$ with A_r as a constant cross section area, g is the gravitational acceleration, and $J_s(Q(z,t),\wp)$ is the hydraulic gradient caused by the friction per unit length. Model (1) is developed by assuming elastic pipes, weakly compressible fluids and with a flow velocity significantly lower than the pressure wave speed; see Chaudhry (2014) and Wylie and Streeter (1978) for details. The internal report (Carrera, 2019) describes the specific procedure used for the calculation of a_1 and a_2 from physical parameters of our installation.

To characterize the hydraulic gradient, various approximation functions with respect to the average flow rate have been suggested. These approximations are suitable for design and nominal analysis, and discussions can be found in most hydraulics textbooks, such as Houghtalen, Akan, and Hwang (2010). Leaks, branches and diverse factors generate deviations in the parameters of this function, and it is then necessary to adjust them in real time for a monitoring system. According to Filion and Karney (2003) the friction models are the dominant error sources in a water network. Here the hydraulic gradient function

$$J_s(Q(z,t),\wp)=\wp Q(z,t)^2 \tag{2}$$

is considered for a turbulent flow and all the physical parameters are concentrated in $\wp$. Thus, this parameter involves the Reynolds number, the viscosity, the roughness, the mean diameter of the conduit and the gravity. This loss function is named quasi steady by the hydraulic community since it is independent of the derivative of the flow velocity and depends only on average flow rate and physical parameters. Fig. 1 shows the experimental variations of the parameter $\wp$ during 24 h for the pilot plant described in the appendix. The real-time experiment is carried out with a constant upstream pressure and the downstream atmospheric discharged pressure. The slow deviation of the parameter is clearly recorded and shows that $\wp$ is not always constant.

To fully establish the fluid dynamics of model (1), boundary conditions at the ends of the pipe and the initial conditions of the variables $Q(z,0)$ and $H(z,0)$, respectively, must be given. For a line of length L, the piezometric heads $H(0,t)$ and $H(L,t)$ are assumed to be boundary conditions without a loss of generality.

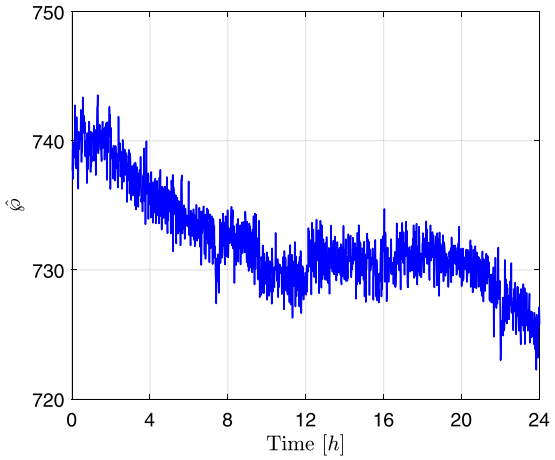

Fig. 1. Variability of $\wp$ during 24 h in the hydraulic pilot plant.

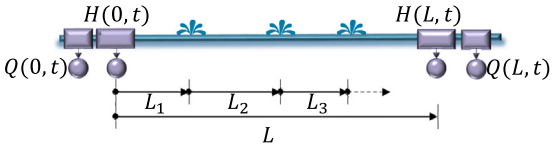

Fig. 2. Leak distribution along the conduit.

The presence of a leak at any arbitrary position $z_e \in (0, L)$ produces a discontinuity in the pair (1), and the additional boundary condition

$$Q(z_e - \epsilon, t) = Q(z_e + \epsilon, t) + \mu(t - \tau)Q_e(t) \tag{3}$$

must be included in the model for each leak, where τ characterizes the leak occurrence instant with $\mu(t)$ as the unit step function, ϵ is an infinitesimal value close to 0 and

$$Q_e(t) = \lambda_e \sqrt{H(z_e, t)} \tag{4}$$

is the outflow rate induced by the piezometric head at the leak point. The parameter λ_e depends on the discharge coefficient, the leak cross section area and the gravitational acceleration and is denoted as leak coefficient in the rest of this work.

Thus, if n leaks are assumed in the line, the fluid model requires an $n + 1$ pair of the form (1) and each pair with its respective boundary condition (3).

By assuming the arbitrarily spatial distribution of n leaks shown in Fig. 2 with $L_0 = 0$ as the reference point, the relation

$$L = \sum_{i=1}^{n+1} L_i \tag{5}$$

characterizes the feasible leakage positions where L_1 and L_{n+1} are defined by the distances from the ends of the conduit to the first and the last leak respectively. The rest of L_is are defined by the separation between the leak $i - 1$ and the leak i for $i = 2, \dots, n$.

For the monitoring of the system, the flow rates at the ends of the pipe are considered as output vector, as consequence,

$$\boldsymbol{y}(t) = [Q(0, t)\ Q(L, t)]'. \tag{6}$$

According to Verde (2001), by applying the finite difference method and by considering n leaks, the minimum finite-dimensional model for (1) can be approximated by

$$\begin{aligned} \dot{Q}(L_i, t) &= \frac{a_1}{L_i}\Big(H(L_{i-1}, t) - H(L_i, t)\Big) - a_1 J_s(Q(L_i, t), \wp), \\ \dot{H}(L_i, t) &= \frac{a_2}{L_i}\Big(Q(L_i, t) - Q(L_{i+1}, t) - \mu_i(t - \tau_i)\lambda_i\sqrt{H(L_i, t)}\Big), \end{aligned} \tag{7}$$

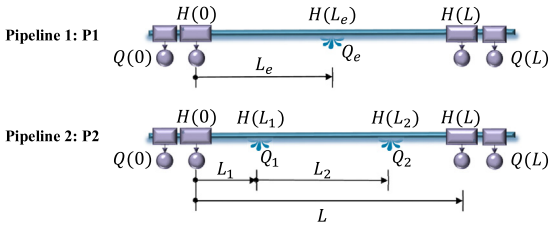

Fig. 3. Variable description of two pipelines with steady state equivalent conditions for one and two leaks. The intermediate flow rate $Q(0) - Q_1$ in the pipeline $P2$.

for $i = 1, \dots, n$ where the intervals L_is satisfy (5) and

$$\dot{Q}(L, t) = \frac{a_1}{L - \sum_{i=1}^{n} L_i}\Big(H(L_n, t) - H(L, t)\Big) - a_1 J_s(Q(L, t), \wp). \tag{8}$$

Thus, the model (7)–(8) with the unknown set of parameters λ_i and L_i allow the formulation of the leakage location task. In this framework, the available real-time observation data are

$$\{Q(0, t),\ Q(L, t),\ H(0, t),\ H(L, t)\}, \tag{9}$$

where the piezometric pressures $H(0, t)$ and $H(L, t)$ correspond to the input of the system.

An interesting property of model (7) for multiple leaks is its input–output equivalent model in steady state with a model in which only one leak is considered. This fact simplifies the diagnosis problem by holding the structure of model (7). The following subsection describes the properties of this model that allows the location of sequential leaks with a pair of switched observers, as it is proposed in Section 3. To simplify the description of the procedure, in the rest of this contribution the time dependence of the variables is omitted without a loss of generality.

2.2. Input–output equivalent models with leaks

The input–output equivalent models that relate the flow in a pipeline with one leak and n leaks were introduced in the book of Korbicz, Koscielny, Kowalczuk, and Cholewa (2004) by assuming a constant friction factor. Fig. 3 describes the flow variables of two pipelines $P1$ and $P2$ with the same parameters a_1 and a_2, the same steady-state pressure heads $H(0)$ and $H(L)$ and flow rates $Q(0)$ and $Q(L)$ at their ends where $Q_e = Q_1 + Q_2$ is satisfied.

Fact 1. Let $P1$ and $P2$ be two pipelines with the same parameters $(a_1, a_2, \wp)$ in normal steady-state conditions as are shown in Fig. 3. In leakage conditions, $P1$ has one leak at distance L_e, and $P2$ has two leaks located at L_1 and L_2, respectively. If leak outflow Q_e is related to

$$Q_e = Q_1 + Q_2 \tag{10}$$

with the outflows Q_1 and Q_2 of $P2$ respectively, according to Verde and Rojas (2017) the leak positions of the two pipelines are related then by

$$\begin{aligned} &\Big(L_e - L_1\Big)\Big(J_s(Q(0), \wp) - J_s(Q(L), \wp)\Big) \\ &\quad = L_2\Big(J_s((Q(0) - Q_1), \wp) - J_s(Q(L), \wp)\Big) \end{aligned} \tag{11}$$

with the hydraulic gradients of the three sections in steady-state. This means the pressure profiles for two leaks and one leak in steady state are indistinguishable at the ends' sections $[0 - L_1]$ and $[L - L_2]$, respectively. These indistinguishability regions justify the necessity of a transitory regime to locate simultaneous leaks. In terms of the parameter λ_1 of the first leak and the piezometric pressure head at the ends of the line, the second leak position can be written by

$$L_2 = \frac{H(L) - H(0) + L_1 J_s\big(Q(0), \wp\big) + (L - L_1)J_s\big(Q(L), \wp\big)}{\wp\Big(Q(0) - \lambda_1\Big[H(0) - L_1 J_s\big(Q(0), \wp\big)\Big]^{1/2}\Big)^2 - J_s\big(Q(L), \wp\big)}. \tag{12}$$

Moreover, by considering (10), the parameter associated with the second leak can be expressed as

$$\lambda_2 = -\frac{Q(0)-Q(L)-\lambda_1\left(H_0-L_1J_s\left(Q(0),\wp\right)\right)^{1/2}}{\left(H(L)+J_s\left(Q(L),\wp\right)(L-L_1-L_2)\right)^{1/2}}, \tag{13}$$

an important inequality of the equivalent model is

$$L_1 < L_e < L_1 + L_2.$$

A property of the equivalent input–output relations (12) and (13) is its generalization to any number of leaks in a recursive way by starting from the two-leak scenario and by knowing the leakage scenario history. ■

From (7) and according to Verde and Rojas (2017), the minimum state–space equivalent model, designed Input–Output Equivalent Model (IO-EM), is given by

$$IO-EM\begin{cases}\dot{Q}(0)=\frac{a_1}{L_e}\left(H(0)-H(L_e)\right)-a_1J_s(Q(0),\wp),\\ \dot{H}(L_e)=\frac{a_2}{L_e}\left(Q(0)-Q(L)-\mu(t-\tau)Q_e\right),\\ \dot{Q}(L)=\frac{a_1}{L-L_e}\left(H(L_e)-H(L)\right)-a_1J_s(Q(L)\wp),\end{cases} \tag{14}$$

where an equivalent outflow Q_e at equivalent position L_e is assumed. This structure with the output vector (6) has the following properties:

Property 1: If $\wp$, L_e and Q_e are known, the system has the strictly linked upper and lower Hessenberg (SLULH) structure. In addition, it is upper and lower measured. Because of these facts, it is observable.

Property 2: It is linear in the known input vector $(H(0), H(L))'$.

Property 3: If $Q_e = 0$ with $0 < L_e < L$, for any bounded input vector with $H(0) > H(L)$, there is only one stable operation point given by

$$Q(0) = Q(L), \qquad H(L_e) = H(0) - \frac{L_e}{L}(H(0) - H(L))$$

and $H(0) > H(L_e) > H(L)$.

Property 4: If $Q_e >= 0$ and $0 < Le < L$ are known signals, the system can be expressed as a nonlinear regressor where the parameter $\wp$ can be identified.

Property 5: If the input vector is locally regular, according to Torres, Besançon, and Georges (2012), an observer can be designed for the augmented system by adding the variables $\wp$, Q_e and L_e as states. Note that the locally regular input imposes a persistent excitation condition that is not acceptable in oil pipelines.

Property 6: If $\wp$ is known, the state and L_e can be reconstructed without the persistent excitation condition.

These properties play an important role for the leak detection proposal presented here. Therefore, if the operation point of the IO-EM does not change simultaneously with a leak, this model with the output vector (6) allows the formulation of three tasks:

- The generation of a residual different from 0 if the parameters L_e and $H(L_e)$ are changed because of an alteration of the leak scenario.
- The identification of $\wp$ associated with the slow variation of the hydraulic gradient with an adaptive observer scheme if L_e is known.
- The reconstruction of the equivalent leak $(L_e, H(L_e))$ by assuming $\wp$ constant with an observer during the time reconstruction.

3. Multiple leakages scheme with hydraulic gradient update

By considering the properties of the IO-EM, the sequential multiple leaks' location can be formulated as a shared task by two observers that work at different time intervals. One updates the hydraulic gradient parameter $\hat{\wp}$ during the detection stage; the other estimates the specific equivalent leak $(\hat{L}_e, \hat{H}_e)$ together with λ_e during the location stage. Thus, these estimations allow the calculation of the physical parameters of the last leak from the previous leakage history by using recursively (12) and (13). The following subsection introduces the proposal scheme with two observers such that the entire multiple leaks' diagnosis is achieved sequentially.

3.1. Architecture

By assuming n sequential leaks of the whole system (7) and by considering the properties (from P1 to P6) of the IO-EM, the problem for leak detection and isolation can be formulated as two estimation tasks that are switched by a binary general residual

$$Ir = \begin{cases} 0 & \text{if the leak has not yet been detected} \\ 1 & \text{if the leak parameters are been estimated,} \end{cases}$$

which controls the detection and location tasks on-line. The proposal algorithm for these tasks is shown in Fig. 4 and consists of four basic functions that are switched according to the residual.

- Gen-Ir: Generate the binary residual Ir from the set of data on-line.
- Idn-$\wp$: If the residual is off, identify the parameter $\hat{\wp}$ of the hydraulic gradient with known L_e. This is feasible by the property P4 of the dynamic of the model IO-EM.
- Rec-L_e: If the residual is on, reconstruct the signal $\hat{L}_e$ and $\hat{H}_e$ with the known parameter $\hat{\wp}$ estimated by the Idn-$\wp$. This is feasible by the property P6 of the dynamic of the model IO-EM. After the reconstruction of the signals, the parameter λ_e is calculated, and the residual turns off.
- Cal-L_i: Calculate the physical parameters of the last leak $\hat{L}_i$ and $\hat{\lambda}_i$ from L_e and λ_e and increment the leak pointer $i = i + 1$. This is feasible by using the relations (12) and (13).

The algorithm starts assuming (14) in the nominal condition with $Ir = 0$, the initial values $\lambda_e = 0$, and $0 < L_e < L$. The sequence of the four tasks can be read as follows:

Detection Stage: By using (14) with L_e and λ_e known, the function Ind-$\wp$ estimates $\hat{\wp}$, and Gen-Ir simultaneously generates Ir. This stage remains so long as the residual is off. When the residual turns on, the value of $\hat{\wp}$ is held, and the algorithm is switched to the Location Stage.

Location Stage: By using (14) with constant $\hat{\wp}$ and adding L_e as states, the estimation of the parameters of the leak and the residual evaluation start. When the parameters converge, the residual Ir turns off, and the update stage starts.

Update Stage: By using the equivalent parameters of the location stage, L_e and λ_e, the physical parameters of the last leak are calculated by (12) and (13). Moreover, the leak pointer is increased by one, and the leak parameters are stored. Thus, the algorithm returns to the detection stage, and it is ready to detect the next leak.

From the scheme proposed in Fig. 4 and the stages' sequence, one can see that the static function Cal-L_i and the switch separate the signals coming from the algorithms Idn-$\wp$ and Rec-L_e. Therefore they can be independently designed. Theoretically, there is not a limitation on the number of sequential leaks that can be located with the above recursive procedure. Since a change of the regime from turbulence to

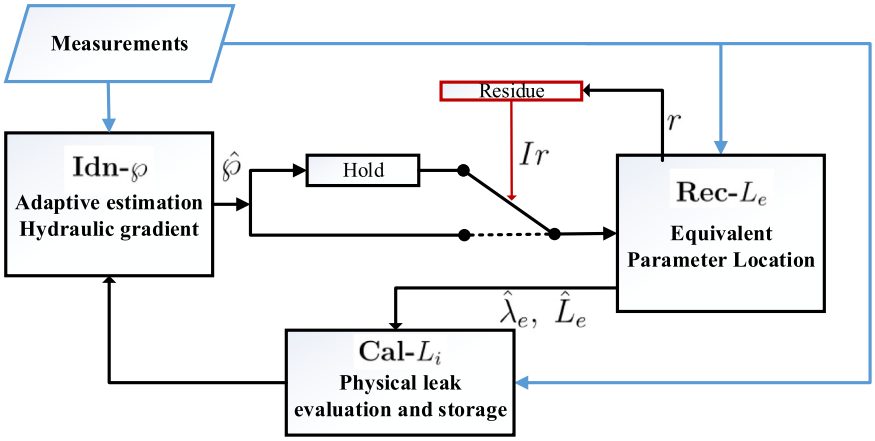

Fig. 4. Switched observers for the location of multiple leaks with hydraulic gradient estimation.

laminar flow invalidates the hydraulic gradient model, a low Reynolds number in leak conditions limits the applicability of the procedure (see Houghtalen et al. (2010)). Note that the minimum time interval between leaks depends on the converge speed of the location stage. The specific dynamic estimator used in the function Rec-L_e determines dominantly the time requires to be in conditions to locate another leak. Two estimators based on the model (14) for this task are described below (EKF and SMO) and both achieve satisfactory convergence time. It is to note that this scheme is more simple in comparison with the method proposed by the authors in Verde and Rojas (2015).

3.2. Adaptive observer for the Idn-$\wp$ task

Fact 2. According to Besançon (2007), a nonlinear system with the structure

$$\dot{\boldsymbol{y}} = \boldsymbol{\alpha}(\boldsymbol{y},\boldsymbol{u},t) + \boldsymbol{\beta}(\boldsymbol{y},\boldsymbol{u},t)\boldsymbol{\theta}(t), \tag{15}$$

with $\boldsymbol{u} \in \mathbb{R}^m$, $\boldsymbol{y} \in \mathbb{R}^p$, and the unknown parameter vector $\boldsymbol{\theta} \in \mathbb{R}^q$, has a particular nonlinear adaptive observer form if

1. $\boldsymbol{y}$ is the measured output variable with $\boldsymbol{e_y} = \hat{\boldsymbol{y}} - \boldsymbol{y}$ as the output error, $\boldsymbol{e_\theta} = \hat{\boldsymbol{\theta}} - \boldsymbol{\theta}$ as the parameter error and $\boldsymbol{e} = [\boldsymbol{e_y}\ \boldsymbol{e_\theta}]^T$.
2. A proper decreasing positive definite C^1 Lyapunov function $V(t,\boldsymbol{e})$ exists, such that for any initial condition $\boldsymbol{y}(0)$, any admissible input $\boldsymbol{u}$, any $t \geq 0$ and any corresponding output solution $\boldsymbol{y}(t)$, one has
$$\frac{\partial V(t,\boldsymbol{e})}{\partial t} \leq -\kappa(\boldsymbol{e}) \tag{16}$$
for some positive definite function $\kappa(\boldsymbol{e})$.
3. $\boldsymbol{\beta}$ is globally bounded and $\boldsymbol{\alpha}$, $\boldsymbol{\beta}$ are globally Lipschitz functions with respect to $(\boldsymbol{y},\boldsymbol{u},t)$, then the function $\kappa(\boldsymbol{e}) = \kappa\|\boldsymbol{e}\|^2$ where $\kappa > 0$.

Moreover, the structure (15) allows the design of adaptive observers on-line with an asymptotic estimation of the state $\boldsymbol{y}$ and of the unknown parameter vector $\boldsymbol{\theta}$. By proposing the Lyapunov function

$$V(t,\boldsymbol{e_y},\boldsymbol{e_\theta}) = \frac{\varepsilon}{2}\boldsymbol{e'_y}\boldsymbol{e_y} + \frac{\varepsilon}{2k_\theta}\boldsymbol{e'_\theta}\boldsymbol{e_\theta} \tag{17}$$

with $\varepsilon > 0$, one can show that

$$\begin{aligned} \dot{\hat{\boldsymbol{y}}} &= \boldsymbol{\alpha}(\boldsymbol{y},\boldsymbol{u},t) + \boldsymbol{\beta}(\boldsymbol{y},\boldsymbol{u},t)\hat{\boldsymbol{\theta}} - k_y(\hat{\boldsymbol{y}} - \boldsymbol{y}); \quad \text{for any scalar} \quad k_y > 0 \\ \dot{\hat{\boldsymbol{\theta}}} &= -k_\theta\boldsymbol{\beta}(\boldsymbol{y},\boldsymbol{u},t)'(\hat{\boldsymbol{y}} - \boldsymbol{y}); \quad \text{for any scalar} \quad k_\theta > 0 \end{aligned} \tag{18}$$

is a state observer for the system (15), in the sense that $\|\boldsymbol{e_y}\|$ goes to 0 as t goes to infinity. Furthermore, if $\boldsymbol{\beta}$ is persistently exciting and $\dot{\boldsymbol{\beta}}$ is bounded, $\|\boldsymbol{e_\theta}\|$ also goes to 0. ■

The adaptive observer (18) is used here to implement the function Idn-$\wp$. By transforming the IO-EM (14) to the canonical adaptive observer form and by assuming as unknown signals $H(L_e)$ and $\wp$, the system takes the form

$$\begin{aligned} \dot{y}_1 &= \frac{a_1}{L_e}u_1 - a_1(y_1^2\theta_1 + \frac{\theta_2}{L_e}), \\ \dot{y}_2 &= \frac{a_1}{L-L_e}u_2 - a_1(y_2^2\theta_1 + \frac{\theta_2}{L-L_e}), \end{aligned} \tag{19}$$

with output $\boldsymbol{y} = \begin{pmatrix} Q(0) & Q(L) \end{pmatrix}'$, input $\boldsymbol{u} = \begin{pmatrix} H(0) & H(L) \end{pmatrix}'$, and the unknown vector $\boldsymbol{\theta} = \begin{pmatrix} \wp & H(L_e) \end{pmatrix}'$.

According to (18), by considering

$$\boldsymbol{\alpha}(\boldsymbol{y},\boldsymbol{u},t) = \begin{pmatrix} \frac{a_1}{L_e}u_1 \\ -\frac{a_1}{L-L_e}u_2 \end{pmatrix} \text{ and } \boldsymbol{\beta}(\boldsymbol{y},t) = \begin{pmatrix} -a_1y_1^2 & -\frac{a_1}{L_e} \\ -a_1y_2^2 & \frac{a_1}{L-L_e} \end{pmatrix},$$

an adaptive observer for (19) can be implemented with $k_y > 0$ and $k_\theta > 0$. As a result, the equilibrium point $\hat{H}(L_e)$ and $\hat{\wp}$ can be updated by this observer.

3.3. Observers for the Rec-L_e task

As indicated in the description of Fig. 4, the leak location consists of the reconstruction of the signal λ_e associated with orifice and its position L_e in (14) every time a new leak is present with an updated $\hat{\wp}$. This means the model

$$\begin{aligned} \dot{x}_1 &= \frac{a_1}{L_e}(u_1 - x_3) - a_1J_s(x_1,\hat{\wp}), \\ \dot{x}_2 &= \frac{a_1}{L-L_e}(x_3 - u_2) - a_1J_s(x_2,\hat{\wp}), \\ \dot{x}_3 &= \frac{a_2}{L_e}(x_1 - x_2 - \lambda_e\sqrt{x_3}), \end{aligned} \tag{20}$$

is the base of the observer with $\boldsymbol{x} = \begin{pmatrix} Q(0) & Q(L) & H(L_e) \end{pmatrix}'$, input $\boldsymbol{u} = \begin{pmatrix} H(0) & H(L) \end{pmatrix}'$, output $\boldsymbol{y} = \begin{pmatrix} Q(0) & Q(L) \end{pmatrix}'$ and the unknown parameters L_e and λ_e.

On the other hand, by considering x_3 as an unknown bounded input signal and the following physical constraints in the steady state

C1: Pressure u_1 is always positive and greater than the unknown pressure head x_3 at the leak position L_e;

C2: The unknown pressure head x_3 at the leak position is always greater than the pressure at the end of the line u_2;

C3: The unknown leak position L_e is always positive and lower than the conduit length L,

diverse unknown input observers can be designed. Two methods have been designed for the equivalent model (20). The first corresponds to the extended Kalman filter (EKF) and the second to the sliding mode (SM) observer taken from Drakunov and Utkin (1995). Both observers allow the residual generation as

$$\delta = |e_1| + |e_2|; \qquad r_{alarm} = \begin{cases} 1 & \delta \geq th \\ 0 & \delta < th, \end{cases} \tag{21}$$

from the estimated output errors $e_1 = Q(0) - \hat{y}_1$ and $e_2 = Q(L) - \hat{y}_2$ and the threshold th is selected according to the procedure reported by Isermann and Münchhof (2006). Taking into account the sensor sensitivity, a minimal outflow of 10% with respect to the nominal flow is considered acceptable. Thus a value of $th = 0.1\bar{Q}$ is used being $\bar{Q}$ the normal mean of flow rate.

3.3.1. Extended Kalman filter (EKF)

The EKF is the extension of the original Kalman filter for a nonlinear system, which is based on the linear time-varying observable system (Gelb, 1994). For a general nonlinear system

$$\begin{aligned} \dot{\boldsymbol{x}} &= \boldsymbol{f}(\boldsymbol{x}, \boldsymbol{u}, t), \\ \boldsymbol{y} &= \boldsymbol{C}\boldsymbol{x} \end{aligned} \tag{22}$$

the extended Kalman filter algorithm corresponds to

$$\dot{\hat{\boldsymbol{x}}} = \boldsymbol{f}(\hat{\boldsymbol{x}}, \boldsymbol{u}, t) + \boldsymbol{K}(t)(\boldsymbol{y} - \hat{\boldsymbol{y}}), \tag{23}$$

$$\hat{\boldsymbol{y}} = \boldsymbol{C}\hat{\boldsymbol{x}} \tag{24}$$

with the Riccati equation

$$\dot{\boldsymbol{P}}(t) = (\boldsymbol{A}(t) + \boldsymbol{I}\eta)\boldsymbol{P}(t) + \boldsymbol{P}(t)(\boldsymbol{A}(t) + \boldsymbol{I}\eta)' + \boldsymbol{Q}_{\boldsymbol{R}} - \boldsymbol{P}(t)\boldsymbol{C}'\boldsymbol{R}^{-1}\boldsymbol{C}\boldsymbol{P}(t), \tag{25}$$

where the time-varying matrix $\boldsymbol{A}(t) = \frac{\partial \boldsymbol{f}(\boldsymbol{x},\boldsymbol{u},t)}{\partial \boldsymbol{x}}$ is evaluated at $\hat{\boldsymbol{x}}$, the pair $(\boldsymbol{A}(t), \boldsymbol{C})$ is observable and the matrices $\boldsymbol{Q}_{\boldsymbol{R}}$ and $\boldsymbol{R}$ are associated with the covariance of the noise into the state and the output vector respectively. Moreover, the parameter $\eta > 0$ in (25) decreases the time of convergence for the estimation (Reif, Sonnemann, & Unbehauen, 1998).

For the particular estimation of L_e and λ_e in (20), the EKF is designed considering that the dynamic of x_3 is faster than the dynamics of x_1 and x_2. This consideration allows the reconstruction of λ_e indirectly from the third equation of (20). This means $\hat{\lambda}_e$ is obtained from

$$0 = \hat{x}_1 - \hat{x}_2 - \hat{\lambda}_e\sqrt{\hat{x}_3},$$

by assuming x_3 is constant. Therefore the identification task can be achieved with the augmented structure

$$\begin{aligned} \dot{\boldsymbol{x}}_{\boldsymbol{a}} &= \boldsymbol{f}_{\boldsymbol{a}}(\boldsymbol{x}_{\boldsymbol{a}}, \boldsymbol{u}, \hat{\wp}), \\ \boldsymbol{y} &= \boldsymbol{C}_{\boldsymbol{a}}\boldsymbol{x}_{\boldsymbol{a}} \end{aligned} \tag{26}$$

with

$$\boldsymbol{x}_{\boldsymbol{a}} = \begin{pmatrix} x_1 & x_2 & x_3 & L_e \end{pmatrix}' \in \mathbb{R}^4, \ \boldsymbol{C}_{\boldsymbol{a}} = \begin{pmatrix} 1 & 0 & 0 & 0 \\ 0 & 1 & 0 & 0 \end{pmatrix} \text{ and}$$

$$\boldsymbol{f}_{\boldsymbol{a}} = \begin{pmatrix} \frac{a_1}{x_{a_4}}(u_1 - x_{a_3}) - a_1 J_s(x_{a_1}, \hat{\wp}) \\ \frac{a_1}{L - x_{a_4}}(x_{a_3} - u_2) - a_1 J_s(x_{a_2}, \hat{\wp}) \\ 0 \\ 0 \end{pmatrix}.$$

where only the unknown parameter L_e is added to (20). This model has the advantage that the dimension of the state has increased only by one state.

Therefore, the EKF algorithm is reduced to

$$\begin{aligned} \dot{\hat{\boldsymbol{x}}}_{\boldsymbol{a}} &= \boldsymbol{f}_{\boldsymbol{a}}(\hat{\boldsymbol{x}}_{\boldsymbol{a}}, \boldsymbol{u}, \hat{\wp}) + \boldsymbol{K}(t)(\boldsymbol{y} - \hat{\boldsymbol{y}}), \\ \hat{\boldsymbol{y}} &= \boldsymbol{C}_{\boldsymbol{a}}\hat{\boldsymbol{x}}_{\boldsymbol{a}}, \end{aligned} \tag{27}$$

where $\boldsymbol{K}(t) = \boldsymbol{P}(t)\boldsymbol{C}'\boldsymbol{R}^{-1}$, $\boldsymbol{P}(t)$ is the solution of (25) obtained with $\eta = 0.5$ and

$$\boldsymbol{A}(t) = \begin{pmatrix} -2a_1\hat{\wp}\hat{x}_1 & 0 & -\frac{a_1(u_1 - \hat{x}_3)}{\hat{L}_e^2} & -\frac{a_1}{\hat{L}_e} \\ 0 & -2a_1\hat{\wp}\hat{x}_2 & -\frac{a_1(u_2 - \hat{x}_3)}{(L - \hat{L}_e)^2} & \frac{a_1}{L - \hat{L}_e} \\ 0 & 0 & 0 & 0 \\ 0 & 0 & 0 & 0 \end{pmatrix},$$

$$\boldsymbol{Q}_{\boldsymbol{R}} = \begin{pmatrix} 1 \times 10^{-1} & 0 & 0 & 0 \\ 0 & 1 \times 10^{-1} & 0 & 0 \\ 0 & 0 & 1 \times 10^{2} & 0 \\ 0 & 0 & 0 & 1 \end{pmatrix}, \qquad \boldsymbol{R} = 100 \begin{pmatrix} 1 & 0 \\ 0 & 1 \end{pmatrix}.$$

This design, as it is shown in the results section, allowed a satisfactory transient response for the estimation without excessive high weights in the covariance of the unknown state (x_3, x_4).

3.3.2. Sliding mode observer (SMO)

The sliding mode (SM) algorithms are recognized in general as robust; thus, a leak locator based on SMO is tested here to estimate the leak position and the parameter associated with the orifice. In particular, for each output data in the model (20), a SMO is designed.

Fact 3 (*Drakunov & Utkin, 1995*)**.** Let the system

$$\dot{y} = f(y) + \phi(t) \tag{28}$$

with the measurable state $y \in \mathbb{R}$ and the unknown signal $\phi(t)$ be bounded, and let

$$\dot{\hat{y}} = f(y) + \psi(t) \tag{29}$$

be an SMO for (28) with the output error $e_y = y - \hat{y}$.

If the control equivalent signal $\psi(t) = \gamma sign(e_y)$ in the SMO (29) satisfies $\gamma > |\phi(t)|$, the output error e_y converges in finite time to 0. Moreover, according to the equivalent control concept, the corrective term $\psi(t)$ can be replaced on the SM surface by its average equivalent value $\bar{\psi}(t) = (\psi)_{ave}$ calculated by making $\dot{e}_y = 0$ and $e_y = 0$. Therefore, the reconstruction of $\phi(t)$ is achieved by

$$\hat{\phi}(t) = \bar{\psi}(t). \quad \blacksquare$$

By considering the steady state conditions (C1 to C3) of the model (20), one can see that the terms

$$\phi_1 = \frac{a_1}{L_e}(u_1 - x_3) > 0 \qquad \text{and} \qquad \phi_2 = \frac{a_1}{L - L_e}(x_3 - u_2) > 0 \tag{30}$$

are bounded and involve the unknown leak parameters.

Thus, ϕ_1 and ϕ_2 can be independently reconstructed with two SMOs according to Fact 3: one for state x_1 and the other for x_2, respectively, in (20). This means the observers

$$SMO_1: \ \dot{\hat{y}}_1 = -a_1 J_s(y_1, \hat{\wp}) + \psi_1, \tag{31}$$

$$SMO_2: \ \dot{\hat{y}}_2 = -a_1 J_s(y_2, \hat{\wp}) + \psi_2 \tag{32}$$

with $\psi_i = \gamma_i sign(e_{yi})$, the output error $e_{yi} = y_i - \hat{y}_i$ and parameter $\gamma_i > |\phi_i|$ reconstruct the unknown signals

$$\hat{\phi}_i(t) = \bar{\psi}_i(t) \quad \text{for} \ \ i = 1, 2.$$

An advantage of the SM algorithm is that the leak parameters L_e and λ_e can be calculated from the average equivalent signals $\bar{\psi}_1$ and $\bar{\psi}_2$ when the SM surfaces are achieved and $\hat{\wp}$ is assumed known. Thus,

$$\begin{aligned} \hat{L}_e &= \frac{a_1(u_1 - u_2) - \bar{\psi}_2 L}{\bar{\psi}_1 - \bar{\psi}_2}, \\ \hat{x}_3 &= u_1 - \frac{\bar{\psi}_1 \hat{L}_e}{a_1}, \end{aligned} \tag{33}$$

and the leak coefficient can be calculated by

$$\hat{\lambda} = \frac{\hat{y}_1 - \hat{y}_2}{\sqrt{\hat{x}_3}}. \tag{34}$$

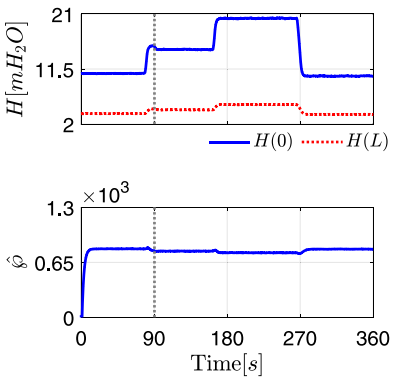

Fig. 5. Evolution of the input data and the estimation of $\hat{\wp}$ with the adaptive observer.

Note from the above equations that the difference between the average equivalent signals ($\bar{\psi}_1$, $\bar{\psi}_2$) must be different from 0 to detect L_e. According to the physical parameters of the pipeline, the gains of the SMOs are selected as $\gamma_1 = \gamma_2 = 0.01$, and the equivalent controls are smoothed with a first order low pass filter of frequency 2 [Hz].

An advantage of the SMO is its finite time convergence. If there is one leak and it disappears at some time, the SMO cannot reconstruct again the normal condition since $\bar{\psi}_1 = \bar{\psi}_2$, unlike the EKF that reconstructs the value $\hat{\lambda}_e = 0$.

4. Experimental results

To independently analyze the performance of the proposed observers, the evolution of each estimator alone is shown first by considering the presence of a leak and changes in the operation point of the upstream pump. The performance of the procedure is tested with real data from the hydraulic pipeline with the configuration described in Appendix A. The implementation of the architecture was made with MATLAB® (MATLAB, 2016).

4.1. Estimation of the hydraulic gradient

To evaluate the performance of the adaptive observer (18) that estimates the parameter $\wp$ associated with the pressure gradient in this experiment, the upstream pressure head produced by the pump was time-variant. For the adaptive observer, the gains $k_y = 5$ and $k_\theta = 10^8$ are used in (18). The changes of the operation point were generated at 79 [s], 162 [s] and 266 [s]. Moreover, at 90 [s] a leakage located at 42.73 [m] from the 0 reference position was provoked by opening a valve with an average outflow rate of $Q_e = 7.5 \times 10^{-4}$ [m^3/s]. The experimental data of the piezometric pressure heads $H(0)$ and $H(L)$ at the ends of the pilot pipeline and the estimated $\hat{\wp}$ are shown in Fig. 5. From the evolution of the input vector $[H(0)\, H(L)]'$ and the estimated parameter $\hat{\wp}$ one can say that the changes of the operation points induce only small deviations in the estimation. This happens, even in the case of a short time interval between an operation point change and the leak occurrence (as example, the interval from 79 [s] to 90 [s]). Thus, the tracing of $\hat{\wp}$ behaves according to the input and the Reynolds number and remains quasi constant during the leak occurrence, as the laws of physics predict. Therefore, the robustness of the adaptive observer as a parameter identifier is proven.

4.2. Location of the equivalent leak

To analyze the behavior of the EKF and SMO as leak locators, a leak placed at 42.73 [m] with an average flow rate of 7.5×10^{-4} [m^3/s] was provoked at 90 [s] together with three upstream pressure head changes in the pilot pipeline. The first two changes occurred at the 79 [s] and at the 162 [s], the last one returns the pump to the initial condition at 266 [s].

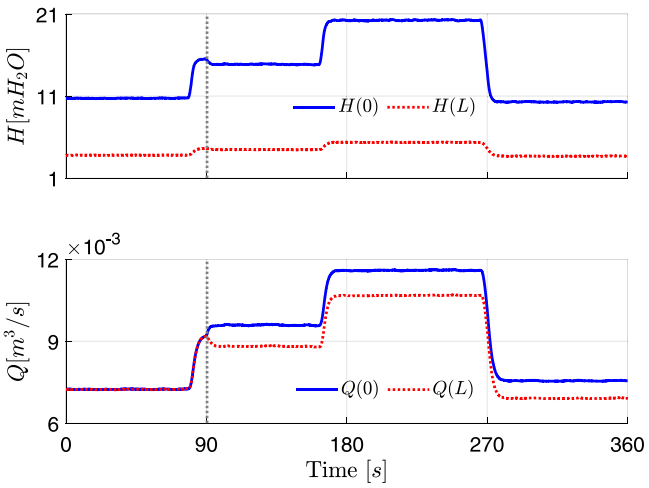

Fig. 6. Experimental data with leaks and operating point changes used in the validation of the EKF and SMO.

Fig. 6 illustrates the data of the pressure head and flow rate at the extremes of the line for this test. Fig. 7 shows the results of the estimated leak position $\hat{L}_e$ and the parameter $\hat{\lambda}_e$ produced by the leak with both observers (EKF and SMO). From the results of both algorithms with the same scenario, the following remarks are established.

- If the SMO is activated in a leakless condition, $\psi_1 = \psi_2$ for any initial condition, there is no reference point for the estimation of the piezometric pressure head $\hat{x}_3$ in (20). As a consequence, the leak position $\hat{L}_e$ (33) was given by the minimal value (0) considered in the implementation. On the contrary, the EKF generated the estimation of $\hat{L}_e$ from the given initial condition of $\hat{x}_4$. Since, the residual is null in this condition with both observers, L_e acts like a dummy variable. With respect to the leak parameter both observers produce a correct value of $\hat{\lambda}_e = 0$.
- When the leak occurs at 90 [s], both observers estimated the unknown signal associated with the leak ($\hat{L}_e$ and $\hat{\lambda}_e$) with a different convergence velocity. The EKF converges slowly in comparison with the SMO (approximately 30 [s]). In favor of both observers, the operation point change produced before the leak (at 79 [s]) does not alter the correct estimations.
- The noise band of the estimations with both algorithms are also different. The chattering band of the SMO induces errors in the leak position $\hat{L}_e$, even if the control equivalent signal is filtered. From a precision point of view, this disadvantage is critical when multiple leaks must be located.
- Both observers remain in the leak position $\hat{L}_e$ and $\hat{\lambda}_e$ even in the presence of changes in the operation point of the system since the parameter of the hydraulic gradient J_s is well known according to the operation point of the experiment. This behavior shows the main benefit of an accurate estimation of $\hat{\wp}$ in real-time.

4.3. Results with the switched observers

The performance of the global location scheme with the EKF is evaluated with a set of two leaks that are generated in the laboratory pipeline by opening two valves at different times and holding the pump with a constant velocity. The first leak was activated at 93.5 [s] and is placed at $L_1 = 42.73$ [m] from reference 0 and the second one was initialized at 195.5 [s] and is located at $L_2 = 56.56$ [m] from L_1. To validate the scheme the relative leak position

$$e_{L_i} = \frac{|L_i - \hat{L}_i|}{L}$$

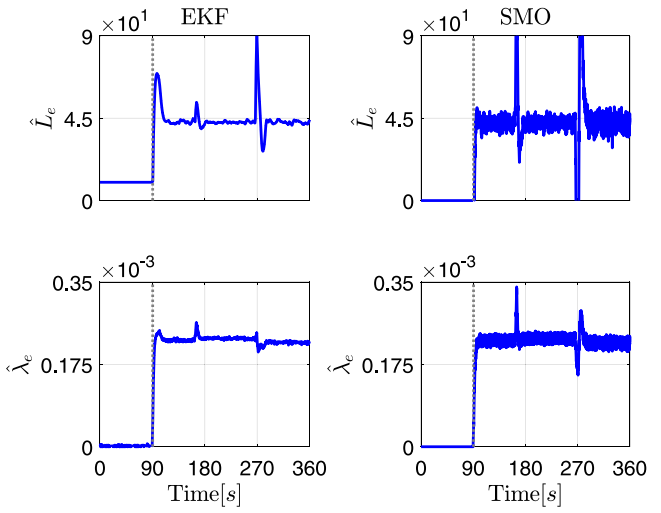

Fig. 7. Evolution of the leak estimation with operating changes by the EKF and SMO.

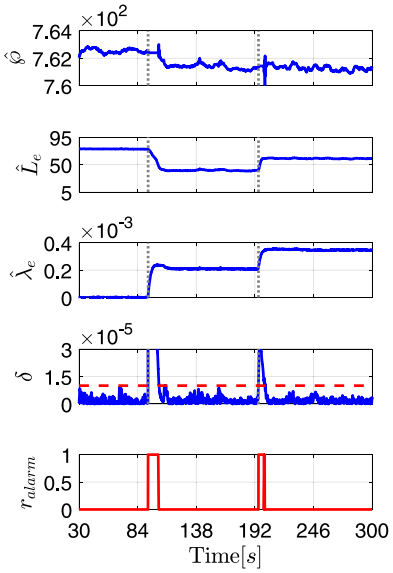

Fig. 8. Evolution of the parameter $\hat{\wp}$, the equivalent leak parameter $\hat{L}_e$ and $\hat{\lambda}_e$ with experimental data of two leaks by the adaptive observer and the EKF.

for each leak is calculated. Also the accumulative error for all the leak scenario $\sum_{i=1}^{2} e_{L_i}$ is evaluated. Since the leak parameter λ_e associated with the coefficient of discharge and the leak area are not yet modeled for the pilot installation, its estimation error is not calculated. An indicator of the accuracy of the spilled flow, the comparison of the estimated equivalent $\hat{Q}_e$ for each leak and the total measured flow rate $(Q(0) - Q(L))$ are analyzed. The physical parameters of the leaks are recursively calculated from $\hat{L}_e$ and $\hat{\lambda}_e$ in the steady-state by (12) and (13) and allow the calculation of the errors e_{L_i}.

Table 1 summarizes the experiment sequence, and the relevant parameters captured during the experiment. The time evolution of leak parameters including the residual δ are shown in Fig. 8. The evolution of the parameter $\hat{\wp}$ throughout the experiment, the pair of parameters $(\hat{L}_e, \hat{\lambda}_e)$ of the equivalent leak and the marks associated with the leak occurrence time are particularly illustrated.

From the table and the time evolution of the estimated parameters the following remarks are established.

- The convergence time of the combined observers is approximately 30 [s]. This time corresponds to the time required to estimate a leak and to be prepared to correctly catch another leak satisfactorily. Thus, from a practical point of view, the time response of the locator is satisfactory.
- The errors in the position e_{L_i} are less than 2%. For a pipeline operator, this parameter is the most critical in a leak monitoring. Thus, from a practical point of view, the satisfactory performance of the locator is validated.
- The equivalent position $\hat{L}_e$ validates again the important inequality $L_1 < L_e < L_1 + L_2$ reported in Verde et al. (2007).
- From the values of the measured mean outflow rate $(Q(0) - Q(L))$ and $\hat{Q}_e$, one can confirm that the virtual variable $\hat{Q}_e$ is an good estimator of the spilled flow by all the leaks.
- The residual δ remains lower than the threshold $th = 10^{-5}$ and the alarm signal r_{alarm} switches the observers.

Table 1
Experiment data and estimation results for two sequential leaks.

Parameter meaning		Leak	
		$i = 1$	$i = 2$
Leak occurrence instant	τ_i [s]	93.5	195.5
Estimated equivalent leak position by EKF	$\hat{L}_e$ [m]	40.52	59.99
Estimated leak position	$\hat{L}_i$ [m]	40.52	55.77
Physical leak position	L_i [m]	42.73	56.56
Relative leak position error in %	$e_{L_i} = \frac{\lvert L_i - \hat{L}_i \rvert}{L}$	1.34%	0.48%
Accumulated position error	$\sum_{i=1}^{2} e_{L_i}$	1.34%	1.82%
Estimated equivalent leak coefficient by EKF	$\hat{\lambda}_e$	2.09×10^{-4}	3.47×10^{-4}
Estimated leak coefficient	$\hat{\lambda}_i$	2.09×10^{-4}	1.40×10^{-4}
Measured outflow rate	$Q(0) - Q(L)$	8.42×10^{-4}	1.29×10^{-3}
Estimated equivalent outflow	$\hat{Q}_e$	8.42×10^{-4}	1.29×10^{-3}
Threshold	th_i	10^{-5}	10^{-5}

Thus, from the above results one can say that if the hydraulic gradient parameter $\hat{\wp}$ is precisely estimated in real time, the equivalent parameters $\hat{L}_e$ and $\hat{\lambda}_e$ allow the reconstruction of sequential leaks in a recursive way with a simple finite dimensional model. This result is coherent with the discussion presented in Rojas and Verde (2018) about the importance of identifying the pressure gradient for diagnosis tasks in pipelines and networks precisely, according to the corresponding estimation stage.

5. Conclusions

This paper proposes a procedure for detecting and locating multiple sequential leaks based on a combination of an adaptive observer, for identifying the hydraulic gradient in real time, and a fault location observer for estimating the position and outflow rate of each leak. The advantage of the scheme is that no additional input excitation is required. The main contribution of this work is the use of an equivalent leak model switched with an identification function for the hydraulic gradient in real time. Moreover, this work shows that the precise knowledge of the hydraulic gradient is a critical point when it comes to leak detection. Experimental results with the data of a pilot pipeline were discussed and showed that the parameters are satisfactorily estimated in spite of operation point changes. Thus, the scheme is promising for the location of sequential leaks occurring in times lapse larger than the approximate 30 [s] for our pipeline installation.

As conclusion, if the parameter $\hat{\wp}$ associated to the hydraulic gradient is correctly estimated in real time, the equivalent parameters $\hat{L}_e$ and $\hat{\lambda}_e$ of a simple finite dimensional model allow the reconstruction of sequential leaks in a recursive way.

It is to remark that theoretically, there is no limitation in the number of sequential leaks that can be located with the above procedure. Practically the magnitude of the outflows and the number of leaks could however limit the applicability of the scheme, since a change of the regime from turbulence to laminar produced by the spilled flow will

Table A.2
Parameters of the pilot pipeline.

Parameters		Values
Pipe diameter	D [m]	0.076
Length of the pipe	L [m]	163.715
Gravitational acceleration	g [m/s^2]	9.81
Fluid pressure wave speed	b [m/s]	1330
Distance between the pumps and the upstream sensors	L_b [m]	1.45
Pipe material		Galvanized iron schedule 40

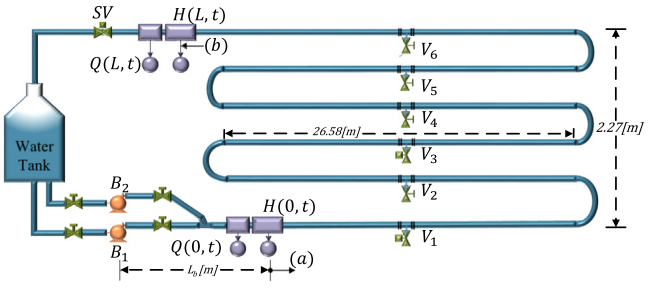

Fig. A.9. Pilot plant scheme at II-UNAM.

invalidate the procedure. The required time to be in conditions to locate another leak depends on the convergence speed of the specific dynamic estimator.

Declaration of competing interest

The authors declare that they have no known competing financial interests or personal relationships that could have appeared to influence the work reported in this paper.

Appendix A. Pilot water pipeline

The pilot water pressurized pipeline located at the Instituto de Ingeniería, UNAM-Mexico is used for the experiments and its layout is shown in Fig. A.9. The material of the pipeline is galvanized iron 40 schedule with a longitude of 163.71 [m] from the points (a) to (b). Physical parameters are reported in Table A.2.

The physical installation consists of a spiral configuration on the vertical plane, the lower part is considered the inlet of the pipeline, where water is supplied with two centrifugal pumps. The outlet is on top of the pipeline that returns the water to the storage tank that has a maximum capacity of 10 [m^3]. Carrera (2019) reported that the U-shapes of the conduit do not considerably modify the total length L if the piezometric head is considered. The pipeline has two flow and two pressure sensors installed one of each at the inlet and the other pair is in the outlet. All data during the experiments was sampled within a period of 100 [ms].

The separation between the pumps and the upstream sensors is $L_b = 1.45$ [m], that is equivalent to almost 20 diameters of the conduit. This distance was adjusted according to the hydraulic handbook (Livelli, 2010) to have a complete developed flow profile in the conduit. A servo valve (SV) was installed in the outlet to restrict the flow when necessary, and 6 valves are available to emulate leaks. In this work, valves $V2$ and $V4$ were used.

Appendix B. Notation

b	Fluid pressure wave speed [m/s]
e_{L_i}	Leak position error
$\boldsymbol{e_y}$	Output error
$\boldsymbol{e_\theta}$	Parameter error
g	Gravitational acceleration [m/s^2]
k_y	Gain constant
k_θ	Gain constant
t	Time variable [s]
th	Residual threshold
$\boldsymbol{u}$	Input vector
$\boldsymbol{x}$	State vector
$\boldsymbol{x_a}$	Augmented state vector
$\boldsymbol{y}$	Output vector
z	Spatial variable [m]
$\boldsymbol{A}$	Jacobian matrix for EKF
A_r	Cross section area [m^2]
$\boldsymbol{C}$	Matrix associated with the measured variables of the model
$\boldsymbol{C_a}$	Augmented matrix associated with the measured variables of the model
D	Pipe diameter [m]
H	Piezometric pressure head [mH$_2$O]
I_r	Binary residual
J_s	Hydraulic gradient
$\boldsymbol{K}$	Gain matrix of the EKF
L	Length of the pipe [m]
L_b	Distance between the pumps and the downstream sensors [m]
L_i	Distance between leaks $i-1$ and i [m]
L_e	Equivalent distance [m]
$\boldsymbol{P}$	Error covariance matrix
Q	Flow rate [m^3/s]
Q_e	Equivalent outflow rate [m^3/s]
$\boldsymbol{Q_R}$	Covariance matrix of the state noise
$\boldsymbol{R}$	Covariance matrix of the output noise
V	Lyapunov function [m^3/s]
γ	Gain constant of the SMO
ε	Infinitesimal value
η	Stability degree for the EKF
τ	Leak occurrence instant [s]
$\boldsymbol{\theta}$	Unknown parameter vector
ϕ	Unknown signal
$\wp$	Parameter of the hydraulic gradient function
$\kappa(\cdot)$	Positive-definite function
κ	Positive-definite constant
λ	Leak coefficient
λ_e	Equivalent leak coefficient
μ	Step function
ψ	Control equivalent signal

References

Ben-Mansour, R., Habiib, M., Kalifa, A., et al. (2012). Computational fluid dynamic simulation of small leaks in water pipelinesfor direct leak pressure transduction. *Computers & Fluids*, 110–123.

Besançon, G. (2007). Parameter/fault estimation in nonlinear systems and adaptive observers. In *Nonlinear observers and applications* (pp. 211–221). Springer.

Besançon, G. (2017). Observer tools for pipeline monitoring. In *Modeling And Monitoring of Pipelines and Networks* (pp. 83–97). Springer International Publishing.

Billman, L., & Isermann, R. (1987). Leak detection methods for pipelines. *Automatica*, *23*(3), 381–385.

Brunone, B., & Ferrante, M. (2001). Detecting leaks in pressurised pipes by means of transients. *Journal of Hydraulic Research*, *39*(5), 539–547.

Carrera, R. (2019). *Prototipo para Detección de Fallas en Tuberías: Manual de Uso. 4a Versión, spanish: Technical report*, Instituto de Ingeniería-UNAM.

Chaudhry, M. C. (2014). *Applied hydraulic transients*. New York: Springer.

Colombo, A. F., Lee, P., & Karney, B. W. (2009). A selective literature review of transient-based leak detection methods. *Journal of Hydro-Environment Research*, *2*, 212–227.

Datta, S., & Sarkar, S. (2016). A review on different pipeline fault detection methods. *Journal of Loss Prevention in the Process Industries*, *41*, 97–106. http://dx.doi.org/10.1016/j.jlp.2016.03.010.

Delgado-Aguiñaga, J. A., Besançon, G., Begovich, O., & Carvajal, J. (2016). Multi-leak diagnosis in pipelines based on extended Kalman filter. *Control Engineering Practice*, *49*, 139–148.

Drakunov, S., & Utkin, V. (1995). Sliding mode observers: Tutorial. In *Proceedings Of the Conference on Decision & Control* (pp. 3376–3378).

Dulhoste, J., Besançon, G., Torres, L., et al. (2011). About friction modeling for observer-based leak estimation in pipelines. In 50th IEEE CDC and European Control Conference (pp. 4413–4418).

Farmer, E. J. (2017). *Detecting leaks in pipelines*. International Society of Automation.

Fernández, H., Verde, C., & Moreno-Pérez, J. (2018). High-order sliding mode observer for outflow reconstruction in a branched pipeline. In IEEE-CCCA (pp. 21–24).

Filion, Y., & Karney, B. (2003). Sources of error in network modeling: A question of perspective. *American Water Works Association*, *95*, 119–130. http://dx.doi.org/10.1002/j.1551-8833.2003.tb10298.x.

Gelb, A. (1994). *Applied optimal estimation*. MIT Press.

Houghtalen, R., Akan, A. O. H., & Hwang, N. H. C. (2010). *Fundamentals of hydraulic engineering systems*. Prentice Hall.

Huang, S., Lin, W., Tsai, M., & Chen, M. (2007). Fiber optic in line distribution sensor for detection on localization of the pipelines leaks. *Sensors Actuators*, *135*, 570–579.

Isermann, R., & Münchhof, M. (2006). *Fault-diagnosis systems*. Springer.

Islam, R., & Chaudhry, H. (1998). Modeling of constituent transport in unsteady flows in pipe networks. *Journal of Hydraulic Engineering*, *124*(11), 115–1124.

Korbicz, J., Koscielny, J., Kowalczuk, Z., & Cholewa, W. (2004). *Fault Diagnosis. Models, Artificial Intelligence, Applications*. Germany: Springer-Verlag.

Lazhar, A., Hadj-Taïeb, L., & Hadj-Taïeb, E. (2013). Two leaks detection in viscoelastic pipeline systems by means of transient. *Journal of Loss Prevention in the Process Industries*, *26*(6), http://dx.doi.org/10.1016/j.jlp.2013.08.007.

Lee, P., Vitkovsky, J., Lambert, M., Simpson, A., & Liggett, J. (2005). Leak location using the pattern of the frequency response diagram in pipelines: a numerical study. *Journal of Sound and Vibration*, *284*(3), 1051–1075. http://dx.doi.org/10.1016/j.jsv.2004.07.023.

Livelli, G. (2010). Flowmeter piping requirements. URL www.flowcontrolnetwork.com/flowmeter-piping-requirements/.

Malekpour, A., & Karney, B. (2018). Reflections on the accoustiic wave propagation speed in homogeneous two-phase flow. In 3th international conference on pressure surges (pp. 455–470).

Martini, A., Troncossi, M., & Rivola, A. (2017). Leak detection in water fillled small diameter polyethylens pipes by mean of acoustic emission measurements. *Applied Sciences*, *7*(2), http://dx.doi.org/10.3390/app7010002.

MATLAB (2016). version 9.0.0 (R2016a). The MathWorks Inc. Natick, Massachusetts.

Puig, V., Ocampo-Martínez, C., Pérez, R., Cembrano, G., Quevedo, J., & Escobet, T. (2017). *Real-time monitoring and operational control of drinking-water systems*. Springer,

Reif, K., Sonnemann, F., & Unbehauen, R. (1998). An EKF-based nonlinear observer with a prescribed degree of stability. *Automatica*, *34*(9), 1119–1123.

Rojas, J., & Verde, C. (2018). On-line head loss identification for monitoring of piplines. In IFAC PapersOnLine 51-24 (pp. 748–754).

Rui, Z., Han, G., Zhang, H., Wang, S., Pu, H., & Ling, K. (2017). A new model to evaluate two leak points in a gas pipeline. *Journal of Natural Gas Science and Engineering*, 491–497.

Torres, L., Besançon, G., & Georges, D. (2012). EKF-like observer with stability for a class of nonlinear systems. *IEEE Transactions on Automatic Control*, *57*(6), 1570–1574. http://dx.doi.org/10.1109/TAC.2011.2175069.

Torres, L., & Verde, C. (2018). Nonlinear estimation of a power law for the friction in a pipeline. In IFAC-on Line (51-13) (pp. 67–72).

Verde, C. (2001). Multi-leak detection and isolation in fluid pipelines. *Control Engineering Practice*, *9*, 673–682.

Verde, C. (2003). Reconfigurable model for multi-leak location in a pipeline. In Proceedings of the American control conference, vol. 4 (pp. 3065–3070).

Verde, C. (2017). Introduction. In *Modeling and monitoring of pipelines and networks* (pp. 1–12). Springer.

Verde, C., Molina, L., & Torres, L. (2014). Parametrized transient model of a pipeline for multiple leaks location. *Journal of Loss Prevention in the Process Industries*, *29*, 177–185.

Verde, C., & Rojas, J. (2015). Iterative scheme for sequential leaks location. *IFAC-PapersOnLine*, *28*(21), http://dx.doi.org/10.1016/j.ifacol.2015.09.613.

Verde, C., & Rojas, J. (2017). Recursive scheme for sequentical leaks' identification. In *Modeling and monitoring of pipelines and networks* (pp. 125–146). Springer.

Verde, C., Visairo, N., & Gentil, S. (2007). Two leaks isolation in a pipeline by transient response. *Applied Water Resources*, *30*, 1711–1721.

Wang, X. (2018). Identification of multiple leaks in pipeline: Linearized model, maximum likelihood, and super-resolution localization. *Mechanical Systems and Signal Processing*, *107*, 529–548.

Wylie, E. B., & Streeter, V. (1978). *Fluid Transients*. McGraw-Hill International Book Co.